Growth-inhibitory Effects of CD40 Ligand (CD154) and Its Endogenous Expression in Human Breast Cancer

Alex W. Tong, Maria H. Papayoti, George Netto, et al.

Clin Cancer Res 2001;7:691-703. Published online March 1, 2001.

Growth-inhibitory Effects of CD40 Ligand (CD154) and Its Endogenous Expression in Human Breast Cancer[1]

Alex W. Tong,[2] Maria H. Papayoti, George Netto, Drew T. Armstrong, Guido Ordonez, J. Mark Lawson, and Marvin J. Stone

Cancer Immunology Research Laboratory [A. W. T., M. H. P., D. T. A., G. O., J. M. L., M. J. S.] and Department of Pathology [G. N.], Baylor-Sammons Cancer Center, Baylor University Medical Center, Dallas, Texas 75246

ABSTRACT

CD40 binding produces multifaceted growth signals in normal and malignant B cells, whereas its physiological role is less well characterized in epithelial cancers. We examined the growth outcome of CD40 ligation in human breast cancer cells, using CD40$^+$ (T47D and BT-20) and CD40-negative (MCF-7, ZR-75–1) cell lines as defined by flow cytometric analysis, immunohistochemistry, and reverse transcription-PCR. Treatment with the soluble recombinant CD40 ligand (CD40L) molecules gp39 or CD40L-trimer significantly reduced [^{3}H]thymidine uptake in BT-20 and T47D cells by up to 40%, but did not affect the growth of CD40-negative MCF-7 or ZR-75–1 cells. Similarly, significant growth inhibition was observed after coincubation with CD40L-transfected murine L cells (55.0 ± 8.9%, $P < 0.001$) that express membrane CD40L constitutively, or with paraformaldehyde-fixed, CD3$^+$ CD40L$^+$ PBLs from three different HLA-mismatched donors (39.7 ± 3.7%, $P < 0.01$). Untransfected L cells and non-CD40L-expressing lymphocytes did not produce significant growth inhibition. The *in vivo* antitumorigenic effects of CD40L were examined using a s.c. severe combined immunodeficient-hu xenograft model. Pretreatment with two different soluble recombinant CD40L constructs (CD40L and gp39) produced similar xenograft growth-inhibitory effects [67 ± 24% ($n = 4$), and 65 ± 14% ($n = 8$) inhibition, respectively], which were reversed by cotreatment with the CD40L-neutralizing antibody LL48. *In vitro* analysis indicated that CD40L-induced growth inhibition was accompanied by apoptotic events including cell shrinkage, rounding, and detachment from the adherent T47D culture monolayer. Thirty-one and 27% of gp39-treated T47D and BT-20 cells underwent apoptosis, respectively, as compared with 56 and 65% from the same cell lines after treatment with the Fas agonistic antibody CH-11. An up-regulation of the proapoptotic protein Bax in T47D and BT-20 cells was observed, which indicated that this Bcl-2 family member may contribute to this growth-inhibitory effect. To explore the clinical relevance of CD40L-CD40 interaction, retrospective immunohistochemical analysis was carried to characterize *in situ* CD40- and CD40L-expression in breast cancer patient biopsies. All of the infiltrating ductal (5 of 5 cases tested) and lobular (4 of 4 cases) breast carcinomas, carcinomas *in situ* (6 of 6 cases), and mucinous carcinoma tested (1 case) expressed CD40. Varying proportions of tumor cells also expressed CD40L in the majority of infiltrating ductal (3 of 5 cases) and lobular (3 of 4 cases) carcinomas, and carcinomas *in situ* (4 of 6 cases), as determined by immunohistochemistry and validated by RT-PCR detection of the CD40L message in only CD40L positive-staining cases. Tumor infiltrating mononuclear cells from infiltrating carcinomas and carcinomas *in situ* expressed CD40 (10 of 10 cases), but less commonly CD40L (1 case of infiltrating lobular carcinoma, 2 cases of carcinoma *in situ*). Our findings indicate that the CD40 signaling pathway is active in human breast carcinoma cells. However, tumor-infiltrating lymphocytes from primary tumor tissues may be limited in their capacity to directly modulate tumor growth through the CD40L-CD40 loop.

INTRODUCTION

Breast cancer is a major health problem in the United States. The >190,000 new cases of breast cancer account for nearly one of every three cancers diagnosed among United States women (1). Breast cancer also ranks second among cancer deaths in women. Conventional treatments of surgery, radiation therapy, chemotherapy, and hormonal therapy produce a long-term survival rate of 56% (2, 3). Recent studies suggest that a variety of biological response modifiers may affect breast cancer cell growth. Cytokines such as TNF[3]-α, IL-6, and transforming growth factor β inhibit BrCa cell growth *in vitro* (3–5). Expression of an *IL-2* transgene also induced breast cancer cell necrosis, an outcome that was correlated with the extent of lymphocytic infiltration (6). Perturbation of the surface HER-2/neu receptor produced objective clinical responses in a recent clinical trial (7). These findings indicate that breast cancer cells are subject to biological and immunological modulation by virtue of specific receptor expression.

Received 8/29/00; revised 11/27/00; accepted 12/8/00.
The costs of publication of this article were defrayed in part by the payment of page charges. This article must therefore be hereby marked *advertisement* in accordance with 18 U.S.C. Section 1734 solely to indicate this fact.
[1] Supported in part by the Tri Delta Cancer Research Fund, the Robert Shanbaum Memorial Fund, and the Edward and Ruth Wilkof Foundation.
[2] To whom requests for reprints should be addressed, at the Cancer Immunology Research Laboratory, Baylor-Sammons Cancer Center, 3500 Gaston Avenue, Dallas, TX 75246. Phone: (214) 820-4123; Fax: (214) 820-2780; E-mail: aw.tong@baylordallas.edu.

[3] The abbreviations used are: TNF, tumor necrosis factor; IL, interleukin; CD40L, CD40 ligand; sCD40L, soluble CD40L; rhsCD40L, recombinant human sCD40L; MAb, monoclonal antibody; PMA, phorbol myristate acetate; PE, phycoerythrin; PBL, peripheral blood lymphocyte; DAB, 3,3′-diaminobenzidine; TSA, tyramide signal amplification; RT, reverse transcription; Tdt, terminal deoxytransferase; TUNEL, Tdt-mediated dUTP nick end labeling; TBS, Tris-buffered saline; SCID, severe combined immunodeficient; BrCa, breast carcinoma; TIL, tumor-infiltrating lymphocyte.

CD40 (M_r 45,000–50,000; 277 amino acids) is a type I transmembrane glycoprotein receptor of the TNF-receptor superfamily. CD40 is best known as a growth signal receptor for B lymphocytes (8–10). Interaction of the $CD40^+$ B cell with an activated, CD40L-expressing T cell (or with sCD40L) produces multifaceted regulatory signals, ranging from T-cell-dependent B-cell proliferation, immunoglobulin production, and immunoglobulin class-switching, to the induction of apoptosis (8, 10–12). The biological outcome depends on maturational stage of the B cell (13–15) and mode of CD40 binding (16–18). Similarly, ligation of CD40 produces diverse physiological functions in a multitude of $CD40^+$ cells that include monocyte/macrophages, T cells, dendritic cells, synovial fibroblasts, and renal tubular epithelial cells (19, 20).

Although CD40 was originally identified in a bladder carcinoma cell line (21), information is limited with regard to its pathophysiological role in epithelial tumors. CD40 is expressed in breast and lung carcinomas and carcinomas of the urinary bladder, nasopharynx, and colon, whereas normal nonproliferating tissues are CD40-negative (22). CD40 ligation induced *in vitro* growth inhibition and/or apoptosis in bladder, ovarian, cervical, and squamous epithelial carcinoma cell lines, as well as in viral-transformed keratinocyte and fibroblast lines (23, 24). Malignant melanoma cells coexpressed CD40 and CD40L, although the pathophysiological role of CD40-CD40L interaction is unclear (25). CD40L inhibited melanoma cell proliferation and induced apoptosis *in vitro* (26), whereas an earlier report suggested that CD40 expression was correlated with a shorter tumor-free survival for malignant melanoma (25).

Recently, we (27) and others (28, 29) demonstrated that CD40 binding modulates human breast cancer cell growth, in which binding with a recombinant sCD40L molecule or with a CD40-reactive MAb produced a direct growth-inhibitory effect. This report confirms our initial findings and demonstrates that multiple forms of sCD40L and membrane-bound CD40L produced similar antitumor outcomes. We also document the expression of CD40L in human breast cancer biopsies. Interestingly, we found that breast cancer TILs, unlike normal activated T lymphocytes, rarely express membrane CD40L and, hence, are limited in their capacity to down-regulate $CD40^+$ breast cancer growth through the CD40 pathway.

MATERIALS AND METHODS

Cell Lines, Antibody, and sCD40L. The human BrCa cell lines (T47D, BT-20, MCF-7, and ZR-75–1), and the myeloma line RPMI 8226 were obtained from American Type Culture Collection. The CD40 antibody MAb89, in unconjugated and PE-conjugated form, and the Fas antibody CH-11 were purchased from Immunotech (Westbrook, ME). The CD40 MAb G28.5 and the recombinant CD40L-CD8 molecule, gp39, were obtained from Dr. Diane Hollenbaugh, Bristol Myers Squibb, Seattle, WA (30). gp39 is a recombinant molecule that contains the human CD40L extracellular domain fused with the murine CD8 extracellular domain. The gp39 monomer has a molecular size of M_r 50,000 and forms dimers and trimers (30). Subsequent studies used gp39 that was generated from Chinese hamster ovary cells transfected with the pME18S plasmid carrying the *gp39* transgene (obtained from Dr. Cees van Kooten, Leiden University, Leiden, the Netherlands; Ref. 9). Biological activity of gp39 was confirmed in our laboratory by lymphoproliferative assays with purified B cells and IL-4 (31). The trimeric human CD40L/leucine-zipper fusion protein (huCD40LT) was obtained from Immunex, Seattle, WA (32). The huCD40LT is a hybrid molecule containing the TNF homologous region of human CD40L incorporated to an isoleucine zipper trimerization motif; with a predicted monomeric molecular size of M_r 20,900 (32). A trimeric recombinant human CD40L (rhsCD40L) was also purchased from Alexis (San Diego, CA). It is a noncovalent trimer beginning at Gly-116 of the human CD40L extracellular region with M_r 48,000 (33). CD40L-transfected L cells were generated as described previously (14). The CD40L antibody LL48 was kindly provided by Dr. Jacques Banchereau (14). All of the human subject-related study protocols were reviewed and approved by the Institutional Review Board for Human Protection at Baylor University Medical Center.

HBL-100 is an epithelial cell line obtained from American Type Culture Collection that was derived from the milk of a nursing mother and contained a tandemly integrated SV40 genome and a type D retrovirus genome. We identified that this cell line expressed CD40 and responded to CD40L growth modulation (see "Results"). However, no additional studies were performed with this virally transformed cell line.

Induction of CD40L Expression in PBLs. For the induction of CD40L expression, peripheral blood mononuclear cells from mismatched donors were obtained by Hypaque-ficoll gradient centrifugation (34) and then treated with PMA (10 ng/ml) and ionomycin (1 μg/ml) at 37° C for 4 h (35). The activated cells were washed (250× g for 7 min), fixed in 1% paraformaldehyde in PBS for 10 min, and washed again before use in coculture studies. CD40L expression was confirmed by flow cytometric direct immunofluorescence analysis, using the CD40L-reactive MAb (clone 89-76) conjugated to PE (Becton Dickinson; San Jose, CA). Two color immunofluorescence analysis with CD3-FITC and CD19-PerCP (Becton Dickinson) indicated that 99% of $CD40L^+$ cells coexpressed the T-cell surface marker CD3.

[^{3}H]Thymidine Uptake Proliferative Assay. [^{3}H]thymidine uptake was used to determine the proliferative activity of BrCa cells after treatment with gp39, huCD40LT, PBLs, or CD40L-transfected L cells. The optimal concentration for each lot of gp39 and huCD40LT was predetermined by B-cell costimulatory and myeloma growth inhibitory assays (16). BrCa cells growing at logarithmic growth phase were trypsinized and resuspended in growth media at 2×10^5cells/ml. One hundred μl of the cell suspension were dispensed onto a 96-well plate. Replicate (three each) samples were incubated with 100 μl of media alone, gp39 (1:8), or huCD40LT (3.0 μg/ml) with or without the leucine-zipper cross-linking antibody M15 (10 μg/ml; Immunex). Alternatively, T47D cells (20,000 cells/well) were dispensed onto a 96-well plate and coincubated with PMA+ionomycin-activated, CD40L-expressing, PBLs seeded at 2×10^4 cells/well. In separate studies, T47D cells were coincubated with irradiated CD40L-L cells (10, 16) or untransfected L-cell adherent monolayers (5×10^3 cells/well). For the neutralization of CD40L response, the CD40L blocking MAb LL48 was added to CD40L-L cells or untransfected L cells at the time of culture. PMA+ionomycin-activated PBLs were

treated with LL48 for 30 min (23°C) prior to the start of culture. The preoptimized LL48 concentration of 10 μg/ml was used in all of the studies (14). In this and previous studies, it has been found that further increase in LL48 (20 μg/ml) did not improve its biological effect. For initial studies with gp39, [^{3}H]thymidine (0.1 μCi/well) was added after 24 or 48 h (37°C, 5% CO_2/95% air). In subsequent studies, breast cancer cells were incubated with huCD40LT for 24 h. Thymidine uptake was determined by liquid scintillation counting after overnight incubation. Growth inhibition was determined by comparing the level of radioisotope uptake (counts per min, or CPM) with untreated cultures by the formula:

$$\% \text{ inhibition} = \left(1 - \frac{CPM_{\text{treated}}}{\text{CPM}_{\text{untreated}}}\right) \times 100\%$$

Immunohistochemical Analysis of CD40 and CD40L Expression. CD40 expression was determined by the immunoperoxidase technique (36). Briefly, the cytospins were fixed in 1% hydrogen peroxide/methanol followed by blocking with normal horse serum. Immunoperoxidase staining involved sequential 60-min incubations at room temperature with the MAb G28.5 (10 μg/ml) or control mouse immunoglobulin, secondary antibody (biotinylated horse antimouse IgG; for 30 min), avidin-biotin-conjugated horseradish peroxidase (Vectastain ABC Elite kit; Vector Laboratories, Burlingame CA; for 35 min), and substrate [3-amino-9-ethylcarbazole (AEC; Biomeda, Foster City CA) or DAB (Vector Laboratories)] with appropriate washings in between. The preparations were counterstained with Meyer's hematoxylin. The frequency of CD40-expressing cells was determined by light microscopy based on the enumeration of 200 cells. For determinations with patient tumor biopsies, formalin-fixed, paraffin-embedded specimens were dewaxed, rehydrated, and quenched in 1% hydrogen peroxide/methanol. The tissue was blocked with normal horse serum followed by incubation with the CD40-reactive MAb89 (1 μg/ml) or control mouse immunoglobulin for 1 h. Subsequent staining steps were performed according to the procedure described above for cytospin samples. The sections were then dehydrated and mounted in nonaqueous mounting media.

CD40L expression in primary tumor specimens was determined by the highly sensitive TSA immunohistochemistry technique (TSA-Indirect kit; NEN Life Science Products, Boston MA). The paraffin-embedded tissue was dewaxed, rehydrated, and quenched in 3% hydrogen peroxide/methanol, then blocked for 30 min. Incubation was carried out for 60 min with the CD40L antibody D-19 (0.5 μg/ml; Santa Cruz Biotechnology, Santa Cruz CA), known to react with CD40L in paraffin-embedded tissues. The tissue was then reacted with a biotinylated rabbit antigoat secondary antibody (Dako, Carpinteria CA; 2 μg/ml, 30 min), streptavidin-horseradish peroxidase (SA-HRP; 30 min), biotinyl tyramide (5 min), and another incubation with SA-HRP (30 min) with washings in between. The substrate DAB (Vector Laboratories) was added (3–5 min), followed by counterstaining with hematoxylin. The tissue was dehydrated and mounted in nonaqueous mounting media. Controls included the use of normal goat IgG as a primary antibody, or CD40L staining without biotinyl tyramide amplification. In addition, PMA+ionomycin-activated PBLs were used as positive controls in initial evaluations. Under optimized conditions, membrane and cytoplasmic staining with the D-19 was demonstrated in 69% of PMA+ionomycin-activated peripheral blood mononuclear cells, whereas control IgG-reacted samples were uniformly negative. Reactivity with CD40 or CD40L was graded by light microscopy by two independent, trained observers (A. W. T., G. N.) based on staining intensity (neg, no staining; +, weak staining; 2+, moderate staining; or 3+, strong staining) and the frequency of reactive cells (rare, <5%; focal, 5–50%; or diffuse, >50%).

RT-PCR. CD40 and CD40L cellular mRNA was detected by the RT-PCR reaction (16) and reverse-transcribed cDNA. Cellular RNA was extracted from cells with the TRIZOL reagent (Life Technologies, Rockville MD). Total RNA was annealed to a sequence-specific 3′ primer and reverse-transcribed with MuLV reverse transcriptase (GeneAmp RNA PCR kit; Perkin-Elmer, Foster City, CA). The reverse-transcription products and PCR reagents were kept at the primer annealing temperature before mixing and the addition of the 5′ and 3′ oligodeoxy-nucleotide primers. Amplification was carried out with AmpliTaq DNA polymerase (denaturing: at 95°C for 1 min and at 94°C for 1 min; annealing: at 56° or 60°C for 45 s; elongation: at 72°C for 1 min; all for 35 cycles). Amplified DNA of the expected size was identified after agarose (1.5%) electrophoresis and ethidium bromide staining. The primer sequences (upstream, 5′-AGAAGGCTGGCACTGTACGA-3′; downstream, 5′-CAGTGTTGGAGCCAGGAAGA-3′) corresponded to residues 365–384 and 769–788, respectively, of the CD40 message and produced a 425-bp CD40-specific DNA amplification product. Concomitant RT and amplification of mRNA for the housekeeping gene β-*actin* mRNA were carried out as an internal positive control.

For detection of the CD40L message in patient tumor biopsies, RNA was extracted from formalin-fixed, paraffin-embedded tissue blocks with the Paraffin Block RNA Isolation kit (Ambion, Austin TX). Tissue sections (20 μm each; 2 sections/case) were deparafinized with xylene (1 ml, 20 min), washed with 100% ethanol (three changes), air-dried, and then digested with proteinase (50°C, 4 h). The samples were washed, suspended in RNA extraction buffer (from kit) for 5 min, treated with acid phenol:chloroform (5 min), and pelleted by centrifugation (12,000 × *g*, 5 min). The aqueous phase was transferred and mixed with 1 μl of linear acrylamide and an equal volume of isopropanol (overnight incubation, −20°C). The RNA was repelleted (13,000 × *g*, 18 min, 4°C) and washed with 75% alcohol (500 μl, 13,000 × *g*, 8 min, 4°C), then air-dried and resuspended in 10 μl of RNA storage solution. To eliminate DNA, the sample was treated with 1 μl of DNase (2 units/μl) in nuclease-free H_2O and DNase I reaction buffer (from kit) for 15 min at 37°C. RNA extraction was repeated with acid phenol: chloroform. The RNA was reprecipitated with isopropanol, linear acrylamide, and 3 M sodium acetate (pH 4.5) for 30 min at −20°C, washed with 75% alcohol, air-dried, then resuspended in 6 μl of RNA storage solution and stored at −20°C. For the RT-PCR reaction, total RNA was annealed to random hexamers and reverse transcribed with MuLV reverse transcriptase (GeneAmp RNA PCR kit; Perkin-Elmer). The reverse-transcription products and PCR reagents were kept at 4°C. Amplification was carried out with AmpliTaq DNA polymerase with an initial denaturation step at 94°C (3 min), followed by 45 cycles of

denaturation (94°C, 30 s), annealing (57°C, 30 s), and elongation (72°C, 30 s). The reaction was terminated after a final elongation step (72°C, 7 min). The amplification product was resolved by agarose (2%) electrophoresis. The primer sequences (upstream, 5′-AATTGCGGCACATGTCATAA-3′; downstream, 5′-GTTTCCCATTTTCCAGGGTT-3′) corresponded to residues 384–403 and 480–499, respectively, of the CD40L message and produced a 116-bp CD40L-specific amplification product. Concomitant RT and amplification of mRNA for the housekeeping gene β-*actin* mRNA were carried out as internal positive control. Dideoxy cycle sequencing reactions were carried out as described previously (16) to verify the molecular identity of the RT-PCR amplification product for the CD40L message. The samples were run on a 310 Genetic Analyzer (Perkin-Elmer). The sequencing data were analyzed bidirectionally and compared with the known sequence for human CD40L cDNA (30).

Quantification of Apoptosis by the TUNEL Assay. A TUNEL method was used to detect DNA fragmentation, with the use of the 96-well apoptosis detection kit TiterTACS (R&D Systems, Minneapolis MN). One hundred μl of T47D cells (1×10^6 cells/ml) were dispensed to each well of a 96-well plate and were reacted with Fas antibody CH-11 (4 μg/ml) or gp39 (1:8) for 24 h. The reactants were washed with PBS ($1000 \times g$, 6 min), fixed with 200 μl of 3.7% buffered formaldehyde solution (10 min), then treated with 100% methanol (20 min) with washings in between. The cells were permeated (CytoPore, 50 μl; 30 min, 23°C), followed by washing with distilled water. Endogenous peroxidase activity was quenched by the addition of H_2O_2 (2.5%, 5 min), washed with distilled H_2O, then treated with Tdt (5 min) and the labeling reaction mix (1 h, 37°C). The cells were treated with a stop buffer (5 min), then streptomycin-horseradish peroxidase (10 min, 23°C), and washed with PBS-0.1% Tween 20. One hundred μl of TACS-Sapphire were added (5 min in the dark), and the reaction was stopped with the addition of 2 N HCl. The colorimetric reaction was quantified as a function of absorbance at 450 nm (SpectraMax 340, Molecular Devices, Sunnyvale, CA). The maximal level of apoptosis was determined by adding 50 μl of TACS-nuclease to T47D cells (1 h, 37°C). Cells treated with the labeling reaction mix without the Tdt enzyme served as a negative control.

Flow Cytometric Detection of CD40 Expression and Annexin V Binding. Direct immunofluorescence analysis was used to determine the frequency of CD40-expressing breast cancer cell lines. Breast cancer cell lines at logarithmic growth phase were trypsinized for 15 (BT-20, HBL-100) or 30 min (T47D, ZR-75–1, MCF-7), washed, and resuspended at 2.5×10^5 cells/ml in PBS containing 1% BSA. Five $\times 10^5$ cells were pelleted, resuspended in 80 μl of PBS, and incubated with 20 μl of the PE-conjugated CD40 antibody MAb89 (12.5 μg/ml) or control mouse MAb for 40 min at 4°C in the dark. The reactants were washed three times with cold PBS+1% BSA, and resuspended with 500 μl of 1% paraformaldehyde in PBS. The frequency of CD40-positive cells was determined by fluorescence-activated cell sorting (FACS) flow cytometric analyses of 5000 events (16) and CELLQuest software analysis (Becton Dickinson). Concomitant analysis of the multiple myeloma cell line RPMI 8226 was carried out as a positive control, in which >90% cells were found to be CD40 positive (16).

Confirmation of apoptotic activity was carried out by quantifying annexin V binding cells (Apoptosis Detection kit; R&D Systems). T47D cells were seeded in a 6-well plate (1×10^6 cells/well) overnight, then treated with medium alone, gp39 (1:4), and/or cyclohexamide (50 μg/ml; Sigma, St. Louis, MO) for 24 h. The cells were trypsinized, resuspended with medium, washed twice in cold PBS, then reconstituted to 1×10^6 cells/ml in binding buffer (from kit). One $\times 10^5$ cells (100 μl) were treated with prediluted fluorescein-labeled annexin V (ANN) and propidium iodide (PI; 10 μl each, 15 min at 23°C) in the dark. Binding buffer (400 μl) was added to each sample prior to two-color immunofluorescence analysis (Becton Dickinson FACScan) with an excitation wavelength at 488 nm. The frequency of ANN+, PI+, and double-positive cell fractions was determined by the proportion of cells with green, red, and double-fluorescent cells in 5000 events, based on CELLQuest software analysis (Becton Dickinson).

Multiprobe RNase Protection Assay. The RNase protection assay (RPA III; Ambion) was used to characterize mRNA expression of the Bcl-2 family of genes (*bcl-x*$_{L/S}$, *bfl-1*, *bik*, *bak*, *bax*, *bcl-2*, and *mcl-1*). Radiolabeled probe to each specific message was synthesized using the hAPO-2 Multi-Probe Template Set (PharMingen, San Diego, CA) and the MAXIscript T7 Transcription kit (Ambion). T47D cells were seeded in a 60 × 15-mm tissue culture dish and allowed to adhere overnight. The cells were treated with medium alone, gp39 (1:4), or gp39+LL48 (10 μg/ml) for 24 h. Cellular RNA was extracted by TRIZOL (Life Technologies, Rockville, MD), and incubated with the radiolabeled probes (7×10^5 cpm) overnight, followed by digestion of the unprotected fragments with RNase (30°C, 45 min). The protected fragments were precipitated with an inactivation/precipitation solution (provided in kit), diluted in loading buffer (95% formamide, 0.025% xylene and bromophenol blue, 18 mM EDTA, 0.025% SDS), and resolved by agarose gel electrophoresis according to the manufacturer's protocol (Quick Point gel; Novex, San Diego, CA). mRNA expression was quantified by densitometric gel band analysis of the autoradiograph. The absorbance for each gel band was determined using the software Scion Image (Scion Corporation) and was normalized to the corresponding densitometric reading for the housekeeping gene *L32*.

Western Blot Analysis. Western blotting was used to characterize Bcl-2 gene family protein expression. BrCa cells at logarithmic growth phase ($2–5 \times 10^6$ per treatment) were treated with medium alone, gp39, or gp39+LL48 for 24 h. Total cell protein lysate was extracted with 0.3–0.4 ml RIPA buffer (PBS with 1% NP40, 0.5% sodium dioxycholate, 0.1% SDS) containing the ATPase inhibitor sodium orthovanadate (184 μg/ml; Sigma), the protease inhibitors phenylmethanesulfonyl fluoride (100 μg/ml; Sigma) and aprotinin (30 μl/ml; Sigma) at 4°C. The protein concentration was determined by the Coomassie Blue (Pierce, Rockford IL) spectrophotometry (SpectraMax 340). Protein extract (18.5–12.2 μg) was mixed at 1:2 (v/v) with electrophoresis sample buffer (1.0 ml of glycerol, 0.5 ml of β-mercaptoethanol, 3.0 ml of 10% SDS, 1–2 mg of bromophenol blue), boiled at 95°C for 3 min, loaded onto a 12% Tris-HCl gel (Bio-Rad, Hercules CA), and electrophoresed for 90–180 min at 100 V (Mini-Protean II; Bio-Rad) alongside a Kaleidoscope molecular size reference marker (Bio-Rad). The samples were transblotted to a nitrocellulose membrane (18 h, 15 V, 4°C), then soaked

Table 1 Growth inhibitory effect of CD40L on human breast cancer cell lines

Cell line	% CD40$^+$ cells[a]	% growth inhibition by[b]	
		huCD40LT	gp39
CD40 positive[c]			
T47D	94.9%	28.5 ± 5.6%[d]	39.8 ± 11.9%[d]
BT-20	96.5%	33.8 ± 5.0%[d]	40.3 ± 8.2%[e]
HBL-100	96.9%	37.0 ± 10.6%[e]	NT[f]
CD40 negative[c]			
ZR-75-1	<1%	<1%	9.7 ± 8.2%
MCF-7	<1%	NT	<1%

[a] Determined by flow cytometric analysis using the PE-conjugated CD40-reactive MAb89.

[b] Determined with huCD40LT (3 μg/ml) with the cross-linking antibody (Ab) M15 (10 μg/ml) or the CD8-CD40L recombinant molecule gp39 (1:8) at 24–48 h postincubation (n = 2–5). Growth inhibition of T47D cells by huCD40LT without M15 was 22.0 ± 7.3% for the same incubation period (24 h). % inhibition = 1 − ($CPM_{treated}$/$CPM_{untreated}$) × 100%; values represent mean ± SD.

[c] As defined by immunohistochemical analysis with >10% positive-staining cells.

[d] $P < 0.001$ by Student's two-tailed t test.

[e] $P < 0.01$ by Student's two-tailed t test.

[f] NT, not tested.

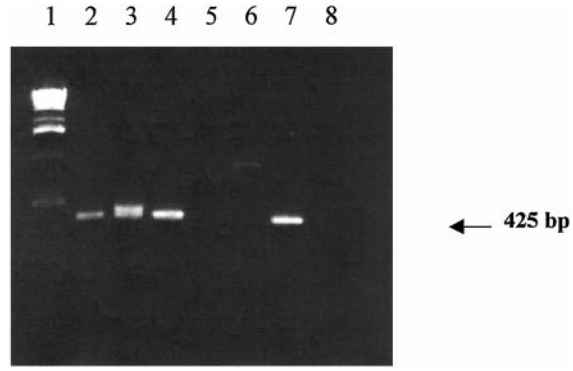

Fig. 1 CD40 expression as determined by RT-PCR. CD40-specific primers were used to generate a 425-bp product by RT-PCR (35 cycles), using RNA extracts from T47D cells (*Lane 2*); HBL-100 (*Lane 3*); BT-20 cells (*Lane 4*); MCF-7 (*Lane 5*); ZR-75–1 (*Lane 6*); ARH-77 myeloma cells (positive control; *Lane 7*); *Lane 1*, molecular size marker; *Lane 8*: no RNA (negative control). HBL-100 is a virally-transformed mammary epithelial cell line that is CD40$^+$ by immunohistochemical analysis.

in 7% milk in TBS and 0.1% Tween 20 for 1 h to block nonspecific binding. Each sample was treated with the appropriate primary antibody (Santa Cruz; 1:10 final dilution, 23°C, 1 h), horseradish peroxidase secondary antibody (1 h; 1:4000 for Bcl 2, and Bax; 1:1000 for β-actin; suspended in 7% milk, 0.1% Tween 20 in TBS) with washings with TBS, 0.1% Tween 20 in between. The membrane was developed by chemiluminescence (Luminol ECL Reagent; Amersham Life Sciences, Buckinghamshire, England) per manufacturer's specifications, and visualized by autoradiography. Semiquantitative analysis was based on densitometric measurements of the reactant bands and normalization to the β-actin reaction in the same lane. Duplicate values differed by ≤10%. Gel bands with A ratios ($A_{protein}$:$A_{\beta\text{-actin}}$) that differed by ≥25% were arbitrarily considered to be significantly different.

BT-20 Xenografts in SCID Mice. The *in vivo* antitumorigenic effect of CD40L was examined using a BT-20 xenograft model in SCID mice (C.B-17/IcrHsd-scid; Harlan Sprague Dawley, Indianapolis IN). BT-20 cells at ~70% confluence were treated for 24 h with medium alone, gp39 from transfected CHO cell cultures, gp39 and the blocking CD40L antibody LL48, control culture supernatant from untransfected CHO cell cultures, or a trimeric soluble recombinant CD40L purchased from Alexis Biochemicals (0.1 μg/ml) in absence of any additional cross-linking agent. Cells were collected after treatment, washed once, then resuspended in RPMI 1640 (1×10^8 cells/ml). Each cell suspension (0.2 ml) was injected into the right flank of each mouse with a 1-ml syringe fitted with a 25-gauge needle. The mice were examined twice weekly for tumor emergence. Tumor size was measured for up to 2 months post-tumor emergence with a Vernier caliper. Mean tumor diameter (D) represents the geometric mean [$D = \sqrt{(D_1 D_2)}$] of two perpendicular measurements (D_1, D_2). The mice were killed and examined for overt tumor metastasis. The primary tumors were also weighed.

RESULTS

CD40 Expression on BrCa Cell Lines. To develop models that are appropriate for the study of CD40-growth regulation, we characterized CD40 expression in established BrCa cell lines by flow cytometric analysis, immunohistochemistry and the RT-PCR technique. Flow cytometric analysis demonstrated that >95% of single cell suspensions from the T47D, BT-20, and BHL-100 lines expressed surface CD40, whereas ZR-75–1 and MCF-7 were CD40 negative (Table 1). Similarly, >80% of total cells in T47D and BT-20 lines expressed CD40 on their membrane surface as defined by immunohistochemical analysis, whereas MCF-7 and ZR-75–1 lines were CD40 negative (<5% positive cells). A 425-bp RT-PCR product corresponding to nucleotides 365–788 of the mature CD40 message was detected only in T47D and BT-20 cells (Fig. 1). Concomitant analysis indicates that the virally transformed mammary epithelial line HBL-100 also expressed CD40. These findings indicated that T47D, and BT-20 lines constitutively expressed CD40 and were suitable for the study of CD40 growth regulation.

Growth Inhibition by sCD40L. Previously, we demonstrated that CD40 is a functional growth-regulatory receptor in myeloma cells (16). Similar evaluations were carried out to examine the role of CD40 in BrCas. Parallel analysis was carried out with two different forms of soluble recombinant CD40L, the recombinant gp39 molecule (a sCD40L-CD8 recombinant molecule obtained from Dr. Hollenbaugh), and huCD40LT, a recombinant fusion protein incorporating three covalently linked extracellular CD40L domains (obtained from Immunex).

The growth inhibitory outcome with optimized concentrations of gp39 and huCD40LT is shown in Table 1. For gp39, no inhibition was observed at a final dilution of 1:32. gp39 (1:8) significantly lowered [^{3}H]thymidine uptake of CD40$^+$ T47D cells by 39.8% ($P < 0.001$; $n = 5$; Table 1) and BT-20 cells by 40.3% ($P < 0.01$; $n = 3$) after 48 h of culture. There was no

significant increase in growth inhibition with a higher concentration (1:2) of gp39 (T47D: 48.3 ± 14.6%, $n = 7$; BT-20: 47 ± 13.5%, $n = 4$). Subsequent analysis showed that comparable levels of growth inhibition were attained within 24 h (38.5 ± 7.1% for T47D cells and gp39 at 1:8; $P > 0.05$ as compared with 48-h cultures). A comparable level of growth inhibition (37%) was observed with the virally transformed, $CD40^+$ mammary epithelial line HBL-100 at 24 h. The same treatment did not significantly alter [^{3}H]thymidine uptake of CD40-negative MCF-7 and ZR-75–1 cells at 24 or 48 h ($P > 0.05$). The trimeric huCD40LT was used at preoptimized concentration (29, 32), which was validated in this laboratory to be 3.0 μg/ml. Like gp39, huCD40LT selectively inhibited the growth of $CD40^+$ breast cancer cells (28.5% for T47D; 33.8% for BT-20 cells; Table 1) in the presence of a cross-linking MAb, M15, at 24 h. In the absence of MAb M15, trimeric CD40L nevertheless induced significant, albeit a lower level of, growth inhibition of T47D cells (22.0 ± 7.3% at 24 h).

Growth Inhibition by Membrane-bound CD40L. The presence of TILs and proinflammatory cells has been correlated with a favorable prognosis for early-onset breast cancer (37, 38). The growth inhibitory effect by exogenous sCD40L raises the possibility that activated CD40L-expressing lymphocytes may participate in antitumor activity via ligation of CD40 on breast cancer cells. We examined this hypothesis by characterizing the antitumor efficacy of normal peripheral blood donor lymphocytes after induction of CD40L expression with PMA+ionomycin (35). Fifty % of peripheral blood mononuclear cells expressed CD40L after this treatment, of which 99% coexpressed the T-cell marker CD3 as defined by flow immunophenotyping analyses.

Treatment with paraformaldehyde-fixed, $CD40L^+$ PBLs from three separate HLA-mismatched, healthy donors resulted in significantly decreased [^{3}H]thymidine uptake of the $CD40^+$ T47D breast cancer cells by 39.7 ± 3.7% ($P < 0.01$; $n = 3$) at 48 h of culture, whereas unactivated lymphocytes from the same donors did not affect breast cancer cell growth (13.8 ± 12.0%; $P > 0.05$; $n = 3$). Similar growth inhibition was observed in three separate experiments by coincubation with irradiated murine L cells that constitutively express membrane-bound CD40L but lacked other surface coactivation molecules that may be expressed on PMA+ionomycin-activated lymphocytes. T47D [^{3}H]thymidine uptake was decreased by 55.0 ± 8.8%, ($P < 0.001$; $n = 3$), whereas untransfected L cells did not (13.3 ± 11.9%; $P > 0.05$; $n = 3$). The growth inhibitory effects by CD40L T lymphocytes or CD40L-expressing L cells were abrogated by pretreatment (for CD40L T cells) or coincubation (for CD40L-L cells) with the CD40L blocking antibody LL48. The results of one of three such experiments are shown in Fig. 2. LL48 alone did not affect breast cancer cell growth ($P > 0.05$; $n = 3$). Together with the finding that multiple HLA-mismatched donors can initiate this CD40-dependent growth-inhibitory event, our observations indicate that peripheral blood T lymphocytes possess the capability of inducing breast cancer growth inhibition via CD40 ligation, an event that is independent of coactivation molecule interaction and HLA compatibility.

Antitumorigenic Effect of CD40L on BT-20 Xenografts in SCID Mice. The *in vivo* antitumorigenic effect of CD40L-induced growth was examined with a BT-20 s.c. xenograft model in SCID mice. Although CD40 binding induced comparable *in vitro* growth inhibition in both $CD40^+$ 47D and BT-20 cells, the maintenance of T47D xenotransplants requires coadministration of estradiol (36), which may affect data interpretation of treatment outcome. Thus heterotransplants were generated using BT-20 cells with or without pretreatment with gp39 prior to tumor inoculation (Fig. 3*A*). Similar studies were carried out with a soluble, trimeric rhsCD40L purchased from Alexis, without further cross-linking per manufacturer's recommendations. Tumor xenografts developed in all untreated ($n = 5$) and mock-treated animals ($n = 8$), and were 10.2 ± 0.7 mm and 6.7 ± 1.5 mm in diameter, respectively, at day 55 postinoculation. By comparison, mean tumor diameter of rhsCD40L- and gp39-treated groups was 3.4 ± 2.4 mm ($n = 4$) and 3.6 ± 1.4 mm ($n = 8$), respectively, at the same time point. Xenograft growth was not evident in one of four mice that received rhsCD40L-treated BT-20 inoculates, and in one of eight animals with gp-39-treated cells. Cotreatment with the CD40L-blocking antibody LL48 abrogated the antitumor effect of gp39 treatment, during which five of five animals developed tumors with a mean diameter of 7.1 ± 1.9 mm (day 55) that did not differ significantly from the untreated group.

To verify that two-dimensional diameter measurements are valid indicators of tumor growth, tumors from various treatment groups were excised and weighed at the time of necropsy. Tumor weights correlated significantly with tumor diameter measurements (Fig. 3*B*) as determined by regression analysis (r, 0.75; $P < 0.001$; $n = 28$). The mean tumor weights of sCD40L-treated animals (139.7 mg) and gp39-treated animals (106.5 mg) were significantly reduced ($P < 0.01$), whereas gp39+LL48-treated tumor weights (362.8 mg) did not differ significantly

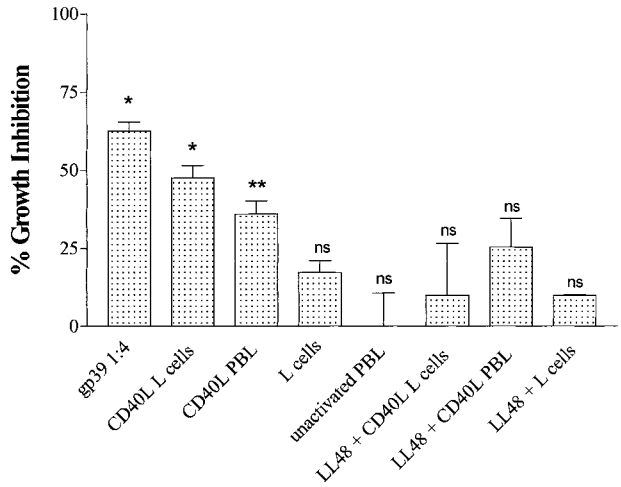

Fig. 2 Growth inhibition by CD40L-expressing cells. T47D cells (2×10^4/well) were dispensed onto a 96-well plate and coincubated with CD40L-expressing, PMA+ionomycin-activated PBLs or unactivated lymphocytes (2×10^4 cells/well), or irradiated CD40L-L cells or untransfected L-cell adherent monolayers (5×10^3 cells/well) with or without the CD40L MAb LL48. Concomitant gp39 treatment was carried out as positive control. Thymidine uptake was determined by liquid scintillation counting after overnight labeling (see "Methods and Materials"). Data shown are from a single representative experiment (mean ± SD). *, $P < 0.05$; **, $P < 0.01$; *ns*, not significantly different from untreated culture by Student's 2-tailed t test ($P > 0.05$).

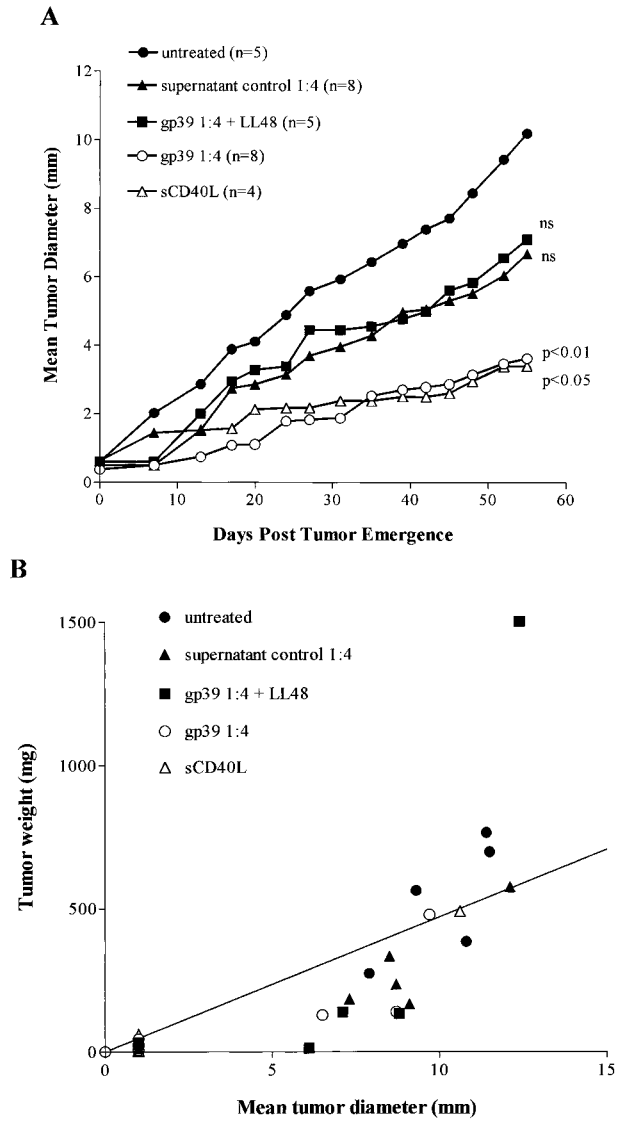

Fig. 3 Antitumorgenic effect of sCD40L. BT-20 breast cancer xenografts were established in SCID mice after *in vitro* treatment with media alone (●), control supernatant from untransfected CHO cell cultures (1:4, ▲), gp39 from transfected CHO cell cultures (1:4, ○), gp39+LL48 (10 μg/ml; ■), or the sCD40L trimer (0.1 μg/ml, △). *A*, mean tumor diameter *versus* time post-tumor emergence; tumor diameter at any given time point was calculated as the geometric mean of two perpendicular caliper measurements. SEs were ≤25% of mean value. Statistical significance was determined by Student's two-tailed *t* test as compared with the untreated mean. *B*, correlation of tumor weight (mg) *versus* mean tumor diameter measurements (mm) at day 55 post-tumor emergence.

from untreated controls (536 mg; $P > 0.05$). At necropsy, local invasion into adjacent tissues was observed in 3 of 18 animals that received either untreated, mock-treated, or gp39+LL48-treated tumor cells. No local invasion was observed in animals that received gp39- or sCD40L-treated xenografts ($n = 12$). These findings are in keeping with the hypothesis that CD40 ligation produces an antitumorigenic effect, resulting in up to 67% decrease in xenograft growth.

Table 2 Induction of apoptosis in breast cancer cells by gp39

Cell line	Treatment[a]	% of maximum apoptotic response[b]
T47D	gp39 1:8	31.1 ± 2.4%[b]
	CH-11	55.9 ± 7.8%
BT-20	gp39 1:8	27.0%[b]
	CH-11	65.1%
ZR-75-1	gp39 1:8	15.2 ± 1.9%
	CH-11	100%

[a] Determined after treatment with a 24-h incubation with CD8-CD40L recombinant molecule gp39 or the agonistic Fas antibody CH-11 (4 μg/ml).

[b] Determined by the TiterTACS ELISA assay which quantifies Tdt labeling of DNA strand breaks. The maximum apoptotic response was established with nuclease-treated cell cultures. % of maximum response = $(A_{\text{treated sample}} - A_{\text{no Tdt}}/A_{\text{nuclease-treated sample}} - A_{\text{no Tdt}}) \times 100\%$; values represent mean ± SD. Apoptotic levels were ≤10% in untreated cultures.

Quantification of Apoptotic Activity. For CD40-transfected carcinoma cells, the ligation of this constitutively expressed growth receptor resulted in growth inhibition and apoptosis (24). Quantification of apoptotic activity by an ELISA-based TUNEL assay showed that gp39-treated T47D and BT-20 cultures had an elevated apoptotic activity that corresponded to 31 and 27% of maximum level, respectively, as compared with 56 and 65% of maximum level after treatment with agonistic Fas antibody CH-11, respectively (Table 2).

Annexin V has a high-avidity binding affinity to negatively charged phospholipids, including phosphatidylserine, which is exposed on the plasma membrane surface of early apoptotic cells (39). There was increased annexin V binding in 23.3 ± 3.79% of gp39-treated cells at 24 h ($n = 4$), an observation that is consistent with elevated apoptotic activity. We observed 46.5 ± 11.2% of annexin V^+ cells with the combined treatment of gp39 and cyclohexamide ($n = 4$), as compared with 22.4 ± 6.91% of cells treated with cyclohexamide alone ($n = 4$). These findings indicate that gp39 growth inhibition was accompanied by apoptosis in BrCa cells, which was further potentiated by simultaneous inhibition of protein synthesis (40).

Alterations in Bcl-2 Family of Proteins after CD40 Binding. Breast cancer cells that undergo chemotherapy or hormone-induced apoptosis display unique patterns of proapoptotic and antiapoptotic expressions (41, 42). The involvement of Bcl-2 family of proteins in CD40-induced apoptosis was characterized with a multiprobe RNase protection assay and Western blot analysis. A multiprobe template set allows simultaneous detection of multiple RNA species in a given sample (*bcl-x_L*, *bcl-x_S*, *bfl-1*, *bik*, *bak*, *bax*, *bcl-2*, *mcl-1*, *L32*, *GAPDH*; RiboQuant hAPO-2 assay). We identified detectable RNA levels for antiapoptotic elements *bcl-x_L* and *mcl1*, and the proapoptotic elements *bcl-x_S*, *bak*, and *bax* in untreated T47D cells (Fig. 4*A*), whereas endogenous *bcl-2* expression was absent. Growth-inhibitory doses of gp39 correspondingly induced a significantly up-regulated level of proapoptotic *bax* (42% increase as compared with untreated) and *bak* (33.3% increase), based on gel band densitometric analysis after normalization to the housekeeping gene *L32* (Fig. 4*A*). This outcome was not observed in cell cultures cotreated with gp39 and LL48 (8 and

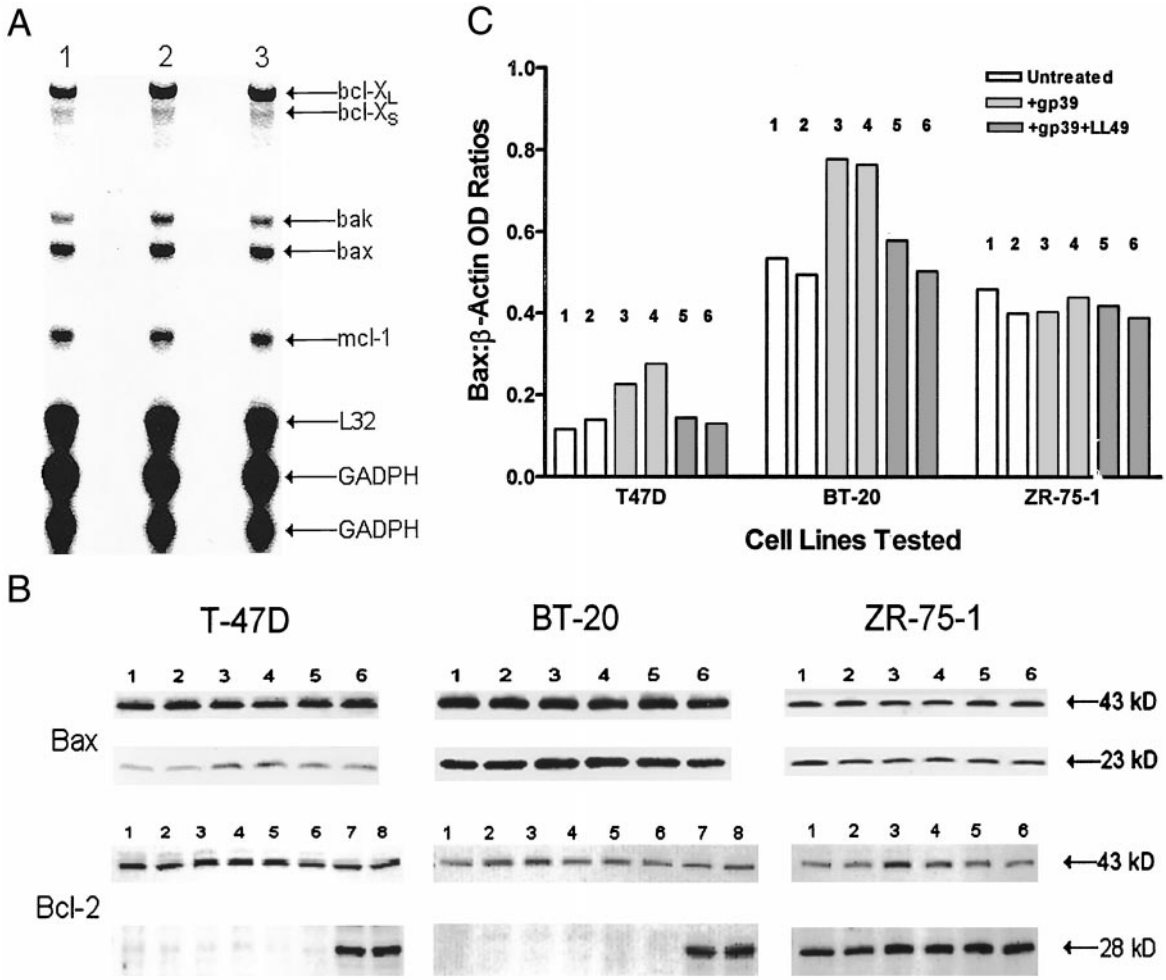

Fig. 4 Expression of Bcl-2 gene family proteins in T47D cells. *A*, mRNA expression of the *Bcl-2* genes was analyzed by the RNase protection assay, using radiolabeled probes specific for *bcl-x*$_L$, *bcl-x*$_S$, *bfl-1, bik, bak, bax, bcl-2, mcl-1, L32,* and *GADPH*, and RNA extracts from T47D cell cultures that were untreated (*Lane 1*), or treated for 24 h with gp39 (*Lane 2*), or gp39+LL48 (10 μg/ml; *Lane 3*). *B*, protein expression of *bax* and *bcl-2* genes was characterized by immunoblot analysis with untreated (*Lanes 1, 2*), gp39-treated (*Lanes 3, 4*), and gp39+LL48-treated (*Lanes 5, 6*) breast cancer cell lines whole-cell protein extract. For the analysis of Bcl-2 expression, positive control reactions (Jurkat cells; *Lanes 7, 8*, with T-47D or BT-20 cell extracts) are also shown. *kD*, M_r in thousands. *C*, densitometric analysis of Bax expression. Bax protein expression was quantified by densitometric analysis and normalized to the corresponding β-actin level (A_{Bax}:$A_{β\text{-}Actin}$) to establish a Bax:β-Actin absorbance ratio. Absorbance ratios for each lane correspond to the gel images shown in *B*.

12% increase, respectively, for *bax* and *bak*, as compared with control; Table 3). By comparison, mRNA levels for *mcl-1* was not significantly altered. *Bcl-x*$_L$ mRNA was also increased after gp39 treatment, but the increase cannot be attributable to a CD40L-specific effect because of its collaterally increased level in LL48+gp39-treated cultures (Fig. 4*A*).

To validate these findings at the protein level, Western blot analysis was carried out using antibodies against Bcl-2 and Bax. (Fig. 4*B*). The proapoptotic protein Bax was significantly elevated (95% for T47D; 50% for BT-20) after gp39 treatment but not in cultures that were treated with gp39 in the presence of LL48 (Fig. 4*C*). Consistent with RNase protection assay findings, CD40-positive T47D and BT-20 cells both lacked Bcl-2 expression before or after gp39 treatment, whereas Bcl-2 was expressed endogenously in the CD40-negative line ZR75–1 and was unaffected by gp39 treatment (Fig. 4*B*). These findings indicate that CD40 growth inhibition correlated with an increased apoptotic activity in breast cancer cells and was accompanied by up-regulation of the proapoptotic *bax.*

CD40 and CD40L Expression in BrCa Patient Biopsies. The *in vivo* growth-inhibitory outcome by exogenous CD40L suggests that endogenous expression of this molecule may potentially serve a growth-regulatory role in human breast cancer. Currently, CD40L expression is undefined within the breast tumor microenvironment. Retrospective immunohistochemical evaluation was carried out to characterize CD40 and CD40L expression in formalin-fixed, paraffin-embedded tumor biopsies (Table 4). Archived primary or metastatic tumor specimens were selected at random from patients with diagnosed breast cancer in 1995. Of the 12 selected biopsy specimens, 5 contained areas of infiltrating carcinoma as well as carcinoma *in situ* by histopathological

Table 3 Effect of CD40L treatment on apoptotic mRNA expression

	A Values						% change *vs.* untreated[b]	
	Absolute			Normalized[a]				
mRNA tested	Untreated	+gp39	+gp39+LL48	Untreated	+gp39	+gp39+LL48	+gp39	+gp39+LL48
bcl-x$_L$	71.3	95.5	98.2	0.13	0.19	0.19	46.2	46.2
bcl-x$_s$	22.2	24.8	23.5	0.04	0.05	0.05	25.0	25.0
bak	30.3	42.5	35.2	0.06	0.09	0.07	33.3	16.7
bax	66.4	85.1	67.1	0.12	0.17	0.13	41.7	8.0
mcl-1	65.8	74.0	61.2	0.12	0.14	0.12	16.7	0
L32	544.8	515.4	514.3					

[a] As determined by the ratio of $A_{\text{test mRNA}}$:A_{L32} from the same cell preparation.
[b] As determined by the formula: normalized *A* value of treated sample/normalized value of untreated sample × 100%.

Table 4 CD40L and CD40 expression in human breast cancer biopsies

		Tumor cell expression[b]		Benign ductal epithelium[b]		Other cell types[c]	
Case ID	Histopathological diagnosis of areas examined[a]	CD40L	CD40	CD40L	CD40	CD40L	CD40
445	Infiltrating ductal Ca,[d] Grade III	+ (f,c)	+ (d,m,c)	+ (f,c)	+ (f,c)	None	TIL, EC
442	Infiltrating ductal Ca, Grade III	+ (d,c)	2+ (d,c)	+ (f,c)	+ (f,c)	MC	TIL, EC
850	Infiltrating ductal Ca, Grade III	neg	3+ (d,c)	neg	+ (f,c)	None	TIL, EC
958	Infiltrating ductal Ca, Grade II	2+ (f,c)	3+ (d,m,c)	neg	2+ (d,c)	None	TIL
511	Infiltrating ductal Ca, Grade I	neg	+ (f,c)	neg	+ (f,c)	None	TIL, EC
762	Infiltrating lobular Ca	+ (f,c)	+ (f,c)	neg	+ (f,c)	TIL	TIL, EC
150	Infiltrating lobular Ca	+ (d,c)	3+ (d,m,c)	neg	+ (f,c)	MC	TIL, EC
481	Infiltrating lobular Ca	neg	2+ (d,m,c)	neg	+ (f,c)	MC	TIL
490	Infiltrating lobular Ca	+/2+ (f,c)	2+ (d,m,c)	neg	+ (f,c)	None	TIL, EC
511	Ductal Ca *in situ*, grade 1	neg	+ (f,c)	neg	+ (f,c)	None	TIL-EC
958	Ductal Ca *in situ*, grade II	2+ (f,c)	2+ (d,m,c)	neg	2+ (f,c)	None	TIL
956	Ductal Ca *in situ*, Grade III	3+ (f,c)	3+ (d,m,c)	n/a	n/a	TIL, MC	TIL, EC
762	Lobular Ca *in situ*	+ (f,c)	+ (d,c)	neg	+ (f,c)	TIL	TIL, EC
150	Lobular Ca *in situ*	+ (d,c)	2+ (d,c)	neg	+ (f,c)	MC	TIL, EC
481	Lobular Ca *in situ*	neg	2+ (d,m,c)	n/a	n/a	MC	TIL
741	Mucinous Ca	2+ (f,c)	2+ (d,c)	neg	+ (f,c)	None	EC
491	LN with metastatic ductal Ca	2+ (d,c)	2+ (d,c)	n/a	n/a	Lymphocytes	Lymphocytes, EC

[a] All are primary breast tissue biopsies except case 491; cases 511, 958, 762, 150, 481 contained infiltrating as well as carcinoma *in situ* by histopathological criteria.
[b] Score represents intensity of staining reaction (see "Methods and Materials"): neg, negative/no staining. Staining pattern: f, focal; d, diffuse; m, membranous; c, cytoplasmic; +, weak staining; 2+, moderate staining; 3+, strong staining.
[c] Cell types indicated were positive for CD40 or CD40L.
[d] Ca, carcinoma; n/a, not applicable, no benign ducts in specimen; EC, endothelial cells; MC, mesenchymal cells; LN, lymph node.

criteria (Table 4). CD40 was expressed unequivocally in 12 of 12 cases, including infiltrating ductal (5 of 5 cases tested) and lobular (4 of 4 cases) subtypes, carcinomas *in situ* (6 of 6 cases), mucinous carcinoma (1 of 1 case), and 1 case of ductal breast cancer metastatic to the lymph node. Ten of 12 cases tested contained >50% of CD40$^+$ breast cancer cells (Table 4). There was complete concordance with respect to the pattern of CD40 expression in all five of the cases that coexpressed infiltrating and *in situ* tumors, although intensity of CD40 staining was noticeably higher in areas of infiltrating carcinoma as compared with regions of *in situ* carcinoma in two cases (case 958 and 150**).** CD40 expression was also observed in the cytoplasm of benign ductal epithelium of biopsy specimens containing CD40$^+$ breast cancer cells (10 of 10 cases; Table 4). In all cases, a focal pattern and lighter staining intensity was observed, which suggested a lower level of CD40 expression as compared with the corresponding malignant cells. A proportion of TILs and endothelial cells were also CD40-positive. These observations extend previous findings (22, 29) and demonstrate that CD40 is commonly expressed in various histological types of breast cancer.

Additional studies were carried out to correlate CD40L expression in the same tumor biopsies by the highly sensitive TSA immunohistochemistry technique. Under optimized conditions, 69% of PMA-ionomycin-activated peripheral blood mononuclear cells expressed CD40L on the membrane and in the cytoplasm, as determined by light -microscopy enumeration of 200 total cells, whereas staining with an irrelevant IgG control was uniformly negative. Concomitant analysis revealed CD40L expression in the cytoplasm of breast cancer cells among the majority of infiltrating ductal (three of five cases), lobular (three of four cases) carcinomas, and carcinomas *in situ* (four of six cases) tested. Compared with CD40 expression,

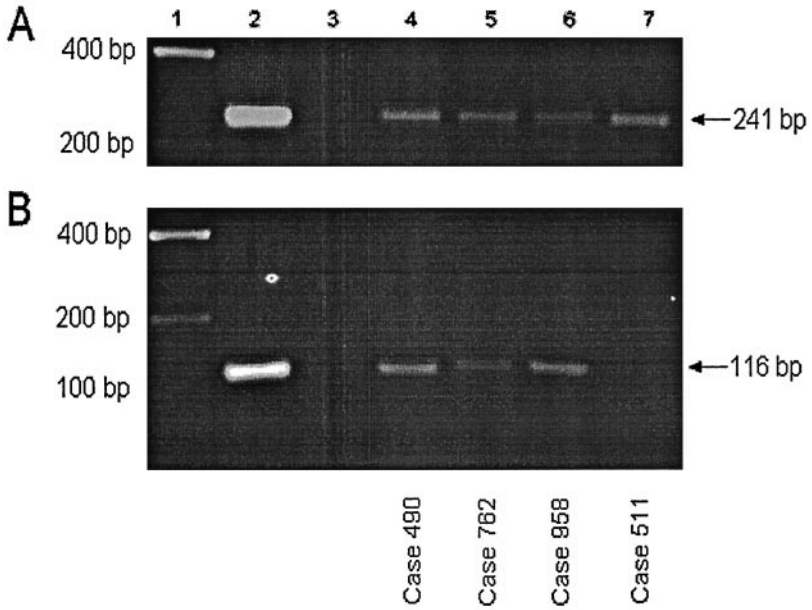

Fig. 5 Detection of CD40L mRNA in breast cancer patient primary tumor biopsy. RT-PCR reactions were carried out to identify the CD40L message in RNA extracts of formalin-fixed, paraffin-embedded primary tumor biopsies that were previously analyzed immunohistochemically for CD40L protein expression. RT-PCR reactions were carried out using specific primers for β-actin (*A*, amplification product of 241 bp) or CD40L (*B*, amplification product of 116 bp) under optimized conditions. *Lane 1*, size markers; *Lane 2*, positive control (CD40L-transfected L cells); *Lanes 3*, negative control (water only as template for RT reaction); *Lanes 4–6*, reactions with RNA from $CD40L^+$ staining samples 490, 762, and 958; *Lane 7*, reactions with RNA from the $CD40L^-$ staining sample 511.

significantly lower proportions of cancer cells expressed CD40L, which was also expressed in mesenchymal cells (Table 4). The pattern of CD40L expression was in complete concordance in areas of infiltrating carcinoma and carcinoma *in situ* for each of the five cases that coexpressed both tumor cell types. By comparison, CD40L expression in benign ductal epithelium was observed in only 2 of 12 cases examined (Table 4).

To verify CD40L expression, RT-PCR analysis was carried out with RNA extracted from the paraffin-embedded tissues and sequence-specific primers corresponding to residues 384–403 and 480–499 of CD40L. RNA was successfully extracted from five of six archived tissue blocks tested, as defined by the capacity to generate a 241-bp β-actin-specific RT-PCR product (Fig. 5). An amplification product corresponding to the residues 384–499 of the open reading frame for CD40L mRNA was successfully generated with RNA extracts from all four of the cases with a positive CD40L immunohistochemical reaction, including case 490, 762, and 958 (*Lanes 3*, *4*, and *5*; Fig. 5). For case 511, which did not express the CD40L protein, the CD40L amplification signal (*Lane 6*) did not exceed background (*Lane 3*, Fig. 5). The cDNA product derived from case 958 was further characterized by RT-PCR cycle sequencing. The bidirectionally analyzed sequence of 5′-AATTGCGGCA CATGTCATAA GTGAGGCCAG CAGTAAAACA ACATCTGTGT TACAGTGGGC TGAAAAAGGA TACTACACCA TGAGCAACAA CTTGGTAACC CTGGAAAATG GGAAAC-3′ was identical to residues 384–499 of the CD40L cDNA open reading frame (30). These findings confirm the expression of CD40L in the limited number of primary breast cancer biopsies tested.

By comparison, tumor infiltrating mononuclear cells from all of the infiltrating carcinomas and carcinomas *in situ* expressed CD40 (10 of 10 cases) but less commonly CD40L (1 case of infiltrating lobular carcinoma, 2 cases of carcinoma *in situ*; Table 4). CD40L may represent a previously unidentified activation marker expressed by TILs (43). The coexpression of CD40L and CD40 is suggestive of an endogenous CD40-growth regulatory mechanism within the breast tumor cell population. Our *in vitro* study indicated that PMA+ionomycin-activated, $CD40L^+$ T lymphocytes can produce a CD40-dependent antitumor effect. However, this activity may be restricted among patient TILs in view of their limited CD40L expression.

DISCUSSION

CD40-CD40L interaction was first shown to play critical roles in B-cell activation and differentiation. Subsequent studies indicated that interaction of the $CD40L^+$ T lymphocyte augments the antigen-presenting function of $CD40^+$ B cells and professional antigen-presenting cells (APCs), which in turn stimulates interacting CD4 and CD8 T cells (8, 19). As expected, CD40 expressed by carcinoma and lymphoma cells have been shown to serve a similar costimulatory role, in which $CD40^+$ tumor cells promote dendritic cell survival (44) and proliferation and differentiation of $CD40L^+$ CTLs (45). Apart from this indirect antitumor effect, there is mounting evidence that the interaction of CD40L with CD40-expressing cancer cells can directly inhibit the growth of multiple myeloma, Burkitt lymphoma, melanoma, and various carcinoma cell types (12, 16, 23, 26, 28, 29, 46, 47).

Our study independently confirmed the recent findings of Wingett *et al.* (28) and Hirano *et al.* (29) that CD40L binding directly inhibits human breast cancer cell growth. Wingett *et al.* (28) showed that IFN-γ preactivation was required for a significant inhibitory effect. Our data are consistent with the findings of Hirano *et al.* (29) that IFN-γ was not a prerequisite for CD40L-induced growth inhibition, although an enhancing effect by this and other cytokines cannot be excluded (29, 47). Different molecules that ligate CD40 may produce different biological outcomes (16, 29). We have used multiple sources of CD40L to validate the direct growth-inhibitory effect, including gp39, a CD40L-CD8 recombinant molecule (30), the trimeric

human CD40L/leucine-zipper fusion protein huCD40LT (32) and the rhsCD40L of similar construct without a leucine-zipper (33). The use of CD40-binding antibodies was excluded in this study, because these antibodies may bind to epitopes that are distinct from those involved in natural CD40-CD40L interaction and trigger a correspondingly different growth signal (10, 15, 48). Discrepancies also have been demonstrated with respect to *in vitro* and *in vivo* growth-inhibitory effects by CD40 MAbs, which may be explained in part by the collateral activation of antibody-dependent cellular cytotoxicity *in vivo* (29). By comparison, we observed a uniform growth-inhibitory effect on CD40-positive breast cancer cell lines by different constructs of sCD40Ls. Conversely, CD40L was ineffective in altering CD40-negative breast cancer cell growth, supporting the critical role of CD40 ligation in this growth-regulatory event.

Both gp39 and sCD40L trimer produced significant, albeit incomplete, tumor growth inhibition *in vitro*. This outcome translated into reductions of *in vivo* human BrCa xenograft growth of 65 and 67%, respectively. Cotreatment with the CD40L-blocking antibody LL48 abrogated this antitumor effect, confirming CD40-dependence of this phenomenon. Although CD40L effectively reduced xenograft progression, it appeared to have a limited capacity to prevent tumor formation. Twenty-five % of animals that received CD40L-treated inoculates (and 12% that received gp39-treated inoculates) failed to develop xenografts. This distribution did not differ significantly from the untreated control group. Additional studies are needed to better characterize the antitumorigenic properties of CD40L. Recent studies have examined the immune-activating effect of CD40L in controlling tumor cell growth (44–46, 49). Our demonstrated direct growth-inhibitory effect *in vitro*, the washing of CD40L-treated tumor cells prior to inoculation, and the immunocompromised phenotype of the nu/nu mouse argue against functional B- or T-cell involvement in the observed *in vivo* antitumor response. However, potential CD40L activation of monocyte/macrophages cannot be excluded, which in turn may produce antitumor cytokines and/or activate natural killer cells (38, 50, 51). Additional studies are planned to characterize the effect of CD40L treatment on a CD40-nonexpressing cell line, to identify or exclude the contribution of immune-activation in CD40L-mediated breast cancer cell growth inhibition *in vivo*.

We found that CD40-dependent growth inhibition triggered events characteristic of apoptosis in breast cancer cells, including exposure of intramembrane phosphotidylserine and increased DNA strand breaks. The level of CD40L-induced apoptosis to be ~one-half of that induced with the agonistic Fas antibody CH-11 and of a similar order of magnitude as growth inhibition measured by [^{3}H]thymidine uptake. These observations are indirect evidence that apoptosis contribute significantly to the CD40L-induced growth inhibitory process. Studies of Binder *et al.* (52), and Rochaix *et al.* (53) showed that 45–75% of BrCas expressed Bax. Our findings of endogenous Bax expression in CD40$^+$ T47-D and BT-20 cells are in keeping with similar observations by others (54). Furthermore, there was a significant up-regulation of this proapoptotic molecule at mRNA and protein levels after CD40 ligation, whereas the CD40L blocking antibody abrogated apoptotic induction and the up-regulation of Bax. Thus, CD40-binding may alter the balance of Bcl-2 family members of apoptotic proteins and trigger apoptosis. Our limited study indicates that the CD40-negative ZR-75–1 cells expressed the antiapoptotic molecule Bcl-2, whereas the CD40$^+$ lines T47D and BT-20 did not. Decreased endogenous Bcl-2 expression was correlated with an increased apoptotic index for breast cancer cases (53). However, these CD40-expressing tumor lines did not appear to be more prone to apoptotic induction by the agonistic Fas antibody CH-11. Additional studies are needed to further characterize the mechanism of CD40-triggered apoptosis, including the possible downstream up-regulation of other TNF-receptor family members (such as Fas, or TNF-related apoptosis-inducing ligand) and/or corresponding caspase activation(s) (55–56). In view of the considerably stronger antitumorigenic effect of CD40L *in vivo* (as compared with measured apoptotic level *in vitro*), other growth-modulatory mechanisms may directly or indirectly contribute to CD40L-induced breast cancer growth inhibition.

In exploring the pathophysiological relevance of CD40L-induced growth inhibition, we have examined CD40 and CD40L expression in patient primary tumor biopsies. We found that all of the breast cancer subtypes tested expressed CD40, including infiltrating ductal and lobular carcinomas and carcinomas *in situ*. It is of interest to note that benign epithelial tissues of these biopsies also exhibited focal, albeit weaker, expression of CD40. These CD40$^+$ benign ductal epithelial tissues are amid or surrounding the malignant tissue and are likely to represent proliferative, albeit benign, epithelial tissues that have been shown previously to express CD40 (22). Additional evaluations of normal, fibrocystic, and hyperplastic specimens are needed to properly define the pattern of CD40 expression in breast epithelium in various states of tumor pathogenesis.

Focal areas of the tumor populations studied also expressed CD40L, which was rarely expressed in benign ductal epithelial tissues in the same cases examined. Only CD40L-positive cases produced a RT-PCR amplification product corresponding to residues 384–499 of CD40L, as verified by dideoxy cycle sequencing. To our knowledge, this is the first report that documents endogenous CD40L expression in BrCa cells. Because only a limited number of cases were examined, further analysis is needed to characterize the relationship, if any, between CD40L expression and tumor grade. The coexpression of CD40L and CD40 is suggestive of a feedback growth loop within the breast cancer population. CD40L was detected primarily within the cancer cell cytoplasm with rare membrane staining, which suggests that expression of the membrane-bound CD40L may be uncommon or occurs transiently (and, hence, escapes detection). Alternatively, cytoplasmic CD40L may represent a precursor of a soluble, biologically active CD40L (57), which has been detected in patients with hematological malignancies (58). In view of the presence of malignant disease despite the potential growth-inhibitory effect of CD40L, we speculate that the CD40L-expressing breast cancer cells may participate in a dynamic, localized growth interactive process. Alternatively, CD40L may represent the outcome of cytokine cascade activation in the tumor microenvironment (51). Prior to the testing of these hypotheses, studies are needed to establish the biological activity of CD40L from patient breast cancer cells.

Our *in vitro* findings indicate that growth inhibition by CD40L$^+$ activated peripheral blood T lymphocytes was mediated at least in part by CD40L-CD40 interactions. Coincubation with LL48 partially abrogated growth inhibition by PMA+ionomycin-activated PBLs. The less than complete reversal may be attributable

to the collateral induction of other members of the TNF family, or other molecules that can regulate breast cancer cell growth (59, 60). Thus, it is of interest that CD40L was infrequently expressed among TILs in the majority of breast cancer cases tested. These findings suggest that TILs in established breast cancers may lack the ability to down-regulate tumor cell growth via CD40L-CD40 interaction, hence favoring tumor progression. Our current analysis does not allow us to further define the cell type expressing CD40 and/or CD40L among the tumor infiltrating mononuclear cells, although the $CD40^+$ subset is likely to represent infiltrating B lymphocytes, macrophages, and dendritic cells (29, 61). The direct antitumor effect by CD40L supports the hypothesis that the stimulation of CD40L expression on breast cancer cells and/or TILs can potentially down-regulate breast cancer cell growth. These approaches are currently being examined in our laboratory. We also plan additional studies with preexisting tumor xenografts that are propagated in a physiologically relevant site such as the mammary fat pad, to confirm the immunotherapeutic potential of sCD40L and/or membrane-bound CD40L. Finally, the relationship of CD40 and CD40L expression with other known surrogate biological prognosticators such as tumor grade and hormonal receptor status (62) will be examined.

ACKNOWLEDGMENTS

We thank Caroline Hunter and Alice Courtney for their technical assistance. We thank Dr. Jacques Banchereau (Baylor Institute for Immunological Research, Dallas, TX) for the supply of the CD40L antibody LL48.

REFERENCES

1. Greenlee, R. T., Hill-Harmon, M. B., Murray, T., and Thun, M. Cancer Statistics, 2001. CA Cancer J. Clin., *51:* 15–36, 2001.

2. Hortobagyi, G. N. Treatment of breast cancer. N. Engl. J. Med., *339:* 974–984, 1998.

3. Burow, M. E., Weldon, C. B., Tang, Y., Navar, G. L., Krajewski, S., Reed, J. C., Hammond, T. G., Clejan, S., and Beckman, B. S. Differences in susceptibility to tumor necrosis factor α-induced apoptosis among MCF-7 breast cancer cell variants. Cancer Res., *58:* 4940–4946, 1998.

4. Eliopoulos, A. G., Stack, M., Dawson, C. W., Kaye, K. M., Hodgin, L., Sihota, S., Rowe, M., and Young, L. S. Epstein-Barr virus-encoded LMP-1, and CD40 mediate IL-6 production in epithelial cells via an NF-κB pathway involving TNF receptor-associated factors. Oncogene, *14:* 2889–2916, 1997.

5. Sovak, M. A., Arsura, M., Zanieski, G., Kavanagh, K. T., and Sonenshein, G. E. The inhibitory effects of transforming growth factor β1 on breast cancer cell proliferation are mediated through regulation of aberrant nuclear factor-κB/Rel expression. Cell Growth Differ., *10:* 537–544, 1999.

6. Stewart, A. K., Lassam, N. J., Quirt, I. C., Bailey, D. J., Rotsein, L. E., Kradjen, M., Dessureault, S., Gallinger, S., Cappe, D., Wan, Y., Addison, C. L., Moen, R. C., Gauldie, J., and Graham, F. L. Adenovector-mediated gene delivery of interleukin-2 in metastatic breast cancer and melanoma: results of a Phase 1 clinical trial. Gene Ther., *6:* 350–363, 1999.

7. Baselga, J., Tripathy, D., Mendelsohn, J., Baughman, S., Benz, C. C., Dantis, L., Sklarin, N. T., Seidman, A. D., Hudis, C. A., Moore, J., Rosen, P. P., Twaddell, T., Henderson, I. C., and Norton, L. Phase II study of weekly intravenous trastuzumab (Herceptin) in patients with HER2/neu-overexpressing metastatic breast cancer. Semin. Oncol., *26* (Suppl. 12)*:* 78–83, 1999.

8. Banchereau, J., Bazan, F., Blanchard, D., Briere, F., Galizzi, J. P., Van Kooten, C., Liu, Y. J., Rousset, F., and Saeland, S. The CD40 antigen and its ligand. Ann. Rev. Immunol, *12:* 881–922, 1994.

9. Van Kooten, C., and Banchereau, J. CD40-CD40L, a multifunctional receptor-ligand pair. Curr. Opin. Immunol., *9:* 330–337, 1997.

10. Miyashita, T., McIlrath, M. J., Grammer, A. C., Miura, Y., Attrep, J. F., Shimaoka, Y., and Lipsky, P. E. Bidirectional regulation of human B cell responses by CD40-CD40 ligand interactions. J. Immunol., *158:* 4620–4633, 1997.

11. Merville, P., Dechanet, J., Desmouliere, A., Durand, I., de Bouteiller, O., Garrone, P., Banchereau, J., and Liu, Y. J. Bcl-2 tonsillar plasma cells are rescued from apoptosis by bone marrow fibroblasts. J. Exp. Med., *183:* 227–236, 1996.

12. Henriquez, N. V., Floettmann, E., Salmon, E., Rowe, M., and Rickinson, A. B. Differential responses to CD40 ligation among Burkitt lymphoma lines that are uniformly responsive to Epstein-Barr virus latent membrane protein 1. J. Immunol., *162:* 3298–3307, 1999.

13. Curnock, A. P., and Knox, K. A. LY294002-mediated inhibition of phosphatidylinositol 3-kinase activity triggers growth inhibition and apoptosis in CD40-triggered Ramos-Burkitt lymphoma B cells. Immunol, *187:* 77–87, 1998.

14. Arpin, C., Dechanet, J., Van Kooten, C., Merville, P., Grouard, G., Briere, F., Banchereau, J., and Liu, Y. J. Generation of memory B cells and plasma cells *in vitro*. Science (Washington DC), *268:* 720–722, 1995.

15. Funakoshi, S., Longo, D. L., Beckwith, M., Conley, D. K., Tsarfaty, G., Tsarfaty, I., Armitage, R. J., Fanslow, W. C., Spriggs, M. K., and Murphy, W. J. Inhibition of human B-cell lymphoma growth by CD40 stimulation. Blood, *83:* 2787–2794, 1994.

16. Tong, A. W., Seamour, B., Chen, J., Su, D., Ordonez, G., Frase, L., Netto, G., and Stone, M. J. CD40 ligand-induced apoptosis is Fas-independent in human multiple myeloma cells. Leuk. Lymphoma, *36:* 543–558, 2000.

17. Pellat-Deceunynck, C., Bataille, R., Robilard, N., Harousseau, J. L., Rapp, M. J., Juge-Morineau, N., Wijdenes, J., and Amlot, M. Expression of CD28 and CD40 in human myeloma cells: a comparative study with normal plasma cells. Blood, *84:* 2597–2603, 1994.

18. Ledbetter, J. A., Grosmaire, L. S., Hollenbaugh, D., Aruffo, A., and Nadler, S. G. Agonistic and antagonistic properties of CD40 Mab G28–5 are dependent on binding valency. Circ. Shock, *44:* 67–72, 1994.

19. Biancone, L., Cantaluppi, V., and Camussi, G. CD40-CD154 interactions in experimental and human disease. Int. J. Mol. Med., *3:* 343–353, 1999.

20. Young, L. S., Eliopoulos, A. G., Gallagher, N. J., and Dawson, C. W. CD40 and epithelial cells: across the great divide. Immunol. Today, *19:* 502–506, 1998.

21. Paulie, S., Rosén, A., Ehlin-Henrikisson, B., Braesch-Andersen, S., Jacobson, E., Koho, H., and Perlmann, P. The human B lymphocyte and carcinoma antigen, Cdw40, is a phosphoprotein involved in growth signal transduction. J. Immunol., *142:* 590–595, 1989.

22. Young, L. S., Dawson, C. W., Brown, K. W., and Rickinson, A. B. Identification of a human epithelial cell surface protein sharing an epitope with the C3d/Epstein-Barr virus receptor molecule of B lymphocytes. Int. J. Cancer, *43:* 786–794, 1989.

23. Eliopoulos, A. G., Dawson, C. W., Mosialos, G., Floettmann, J. E., Rowe, M., Armitage, R. J., Dawson, J., Zapata, J. M., Kerr, D. J., Wakelam, M. J. O., Reed, J. C., Kieff, E., and Young, L. S. CD40-induced growth inhibition in epithelial cells is mimicked by Epstein-Barr virus-encoded LMP-1: involvement of TRAF3 as a common mediator. Oncogene, *13:* 2243–2254, 1996.

24. Hess, S., and Engelmann, H. A novel function of CD40: induction of cell death in transformed cells. J. Exp. Med., *183:* 159–167, 1996.

25. Van den Oord, J. J., Maes, A., Stas, M., Nuyts, J., Battocchio, S., Kasran, A., Garmyn, M., De Wever, I., and De Wolf-Peeters, C. CD40 is a prognostic marker in primary cutaneous malignant melanoma. Am. J. Pathol., *149:* 1953–1961, 1996.

26. Von Leoprechting, A., van der Bruggen, P., Pahl, H. L., Aruffo, A., and Simon, J. C. Stimulation of CD40 on immunogenic human malignant melanomas augments their cytotoxic T lymphocyte-mediated lysis and induces apoptosis. Cancer Res., *59:* 1287–1294, 1999.

27. Papayoti, M. H., Tong, A. W., Banchereau, J., and Stone, M. J. Induction of human breast carcinoma cell apoptosis by CD40-ligand. Proc. Am. Assoc. Cancer Res., *39:* 582, 1998.

28. Wingett, D. G., Vestal, R. E., Forcier, K., Hadjokas, N., and Nielson, C. P. CD40 is functionally expressed on human breast carcinomas: variable inducibility by cytokines and enhancement of Fas-mediated apoptosis. Breast Cancer Res. Treat., *50:* 27–36, 1998.

29. Hirano, A., Longo, D. L., Taub, D. D., Ferris, D. K., Young, L. S., Eliopoulos, A. G., Aganthanggelou, A., Cullen, N., MaCartney, J., Fanslow, W. C., and Murphy, W. J. Inhibition of human breast carcinoma growth by a soluble recombinant human CD40 ligand. Blood, *93:* 2999–3007, 1999.

30. Hollenbaugh, D., Grosmaire, L. S., Kullas, C. D., Chalupny, N. J., Braesch-Andersen, S., Noelle, R. J., Stameknovic, I., Ledbetter, J. A., and Aruffo, A. The human T cell antigen gp39, a member of the *TNF* gene family, is a ligand for the CD40 receptor: expression of a soluble form of gp39 with B cell co-stimulatory activity. EMBO J., *11:* 4313–4321, 1992.

31. Aruffo, A., Farrington, M., Hollenbaugh, D., Milatovich, A., Nonoyoma, S., Bajorath, J., Grosmaire, L. S., Stenkamp, R., Neubauer, M., Roberts, R. L., Noelle, R. J., Ledbetter, J. A., Francke, U., and Ochs, H. D. The CD40 ligand, gp39, is defective in activated T cells from patients with X-linked hyper-IgM syndrome. Cell, *72:* 291–300, 1993.

32. Morris, A. E., Remmele, R. L., Klinke, R., MacDuff, B. M., Fanslow, W. C., and Armitage, R. J. Incorporation of an isoleucine zipper motif enhances the biological activity of soluble CD40L (CD154). J. Biol. Chem., *274:* 418–423, 1999.

33. Pullen, S. S., Labadia, M. E., Ingraham, R. H., McWhirter, S. M., Everdeen, D. S., Alber, T., Crute, J. J., and Kehry, M. R. High-affinity interactions of tumor necrosis factor receptor-associated factors (TRAFs) and CD40 require TRAF trimerization and CD40 multimerization. Biochemistry, *38:* 10168–10177, 1999.

34. Tong, A. W., Zhang, B. Q., Mues, G., Solano, M., Hanson, T., and Stone, M. J. Anti-CD40 antibody binding modulates human multiple myeloma clonogenicity *in vitro*. Blood, *84:* 3026–3033, 1994.

35. Roy, M., Waldschmidt, T., Aruffo, A., Ledbetter, J. A., and Noelle R, J. The regulation of the expression of gp39, the CD40 ligand, on normal and cloned CD4+ T cells. J. Immunol., *151:* 2497–2510, 1993.

36. Moody, T. W., Leyton, J., Unsworth, E., John, C., Lang, L., and Eckelman, W. (Arg^{15}, Arg^{21}) VIP: evaluation of biologic activity and localization to breast cancer tumors. Peptides, *19:* 585–592, 1998.

37. Marrogi, A. J., Munshi, A., Merogi, A. J., Ohadike, Y., El-Habashi, A., Marrogi, O. L., and Freeman, S. M. Study of tumor infiltrating lymphocytes and transforming growth factor-β as prognostic factors in breast carcinoma. Int. J. Cancer, *74:* 492–501, 1997.

38. Camp, B. J., Dyhrman, S. T., Memoli, V. A., Mott, L. A., and Barth, R. J., Jr. *In situ* cytokine production by breast cancer tumor-infiltrating lymphocytes. Ann. Surg. Oncol., *3:* 176–184, 1996.

39. Vermes, I., Haanen, C., Steffens-Nakken, H., and Reutelingsperger, C. A novel assay for apoptosis. Flow cytometric detection of phosphatidylserine expression on early apoptotic cells using fluorescein labelled annexin V. J. Immunol. Methods, *184:* 39–51, 1995.

40. Keane, M. M., Ettenberg, S. A., Lowrey, G. A., Russell, E. K., and Lipkowitz, S. Fas expression and function in normal and malignant breast cells lines. Cancer Res., *56:* 4791–4798, 1996.

41. Zhang, G. J., Kimijima, I., Onda, M., Kanno, M., Sato, H., Watanabe, T., Tsuchiya, A., Abe, R., and Takenoshita, S. Tamoxifen-induced apoptosis in breast cancer cells relates to down-regulation of Bcl-2, but not Bax and Bcl-x(l), without alteration of p53 protein levels. Clin. Cancer Res., *5:* 2971–2977, 1999.

42. Gibson, L. F., Fortney, J., Magro, G., Ericson, S. G., Lynch, J. P., and Landreth, K. S. Regulation of BAX and BCL-2 expression in breast cancer cells by chemotherapy. Breast Cancer Res. Treat., *55:* .107–117, 1999.

43. Lopez, C. B., Rao, T. D., Feiner, H., Shapiro, R., Marks, J. R., and Frey, D. B. Repression of interleukin-2 mRNA translation in primary human breast carcinoma tumor infiltrating lymphocytes. Cell. Immunol., *190:* 141–155, 1998.

44. Esche, C., Gambotto, A., Satoh, Y., Gerein, V., Robbins, P. D., Watkins, S. C., Lotze, M. T., and Shurin, M. R. CD154 inhibits tumor-induced apoptosis in dendritic cells and tumor growth. Eur. J. Immunol., *29:* 2148–2155, 1999.

45. Pericle, F., Epling-Burnette, P. K., Podack, E. R., Wei, S., and Djeu, J. Y. CD40-CD40L interactions provide "third party" costimulation for T cell response against B7–1 transfected human breast tumor cells. J. Leuk. Biol., *61:* 201–208, 1997.

46. Costello, R. T., Gastaut, J. A., and Olive, D. What is the real role of CD40 in cancer immunotherapy? Immunol. Today, *20:* 488–493, 1998.

47. Posner, M. R., Cavacini, L. A., Upton, M. P., Tillman, K. C., Gornstein, E. R., and Norris, C. M., Jr. Surface membrane-expressed CD40 is present on tumor cells from squamous cell cancer of the head and neck *in vitro* and *in vivo* and regulates cell growth in tumor cell lines. Clin. Cancer Res., *5:* 2261–2270, 1999.

48. Bajorah, J., Chalupny, N. J., Marken, J. S., Siadak, A. W., Skonier, J., Gordon, M., Hollenbaugh, D., Noelle, R. J., Ochs, H. D., and Aruffo, A. Identification of residues on CD40 and its ligand which are critical for the receptor-ligand interaction. Biochemistry, *34:* 1833–1844, 1995.

49. Kikuchi, T., and Crystal, R. G. Anti-tumor immunity induced by *in vivo* adenovirus vector-mediated expression of CD40 ligand in tumor cells. Hum. Gene Ther., *10:* 1375–1387, 1999.

50. Grewal, I. S., and Flavell, R. A. CD40 and CD154 in cell-mediated immunity. Ann. Rev. Immunol., *16:* 111–155, 1998.

51. Basolo, F., Calvo, S., Fiore, L., Serra, C., Conaldi, P. G., Falcone, V., Morganti, M., Squartini, F., and Toniolo, A. Production of cytokines and response to them in normal and transformed human mammary epithelial cells. Ann. NY Acad. Sci., *698:* 126–130, 1993.

52. Binder, C., Marx, D., Binder, L., Schauer, A., and Hiddemann, W. Expression of Bax in relation to Bcl-2 and other predictive parameters in breast cancer. Ann. Oncol., *7:* 129–33, 1996.

53. Rochaix, P., Krajewski, S., Reed, J. C., Bonnet, F., Voigt, J. J., and Brousset, P. *In vivo* patterns of Bcl-2 family protein expression in breast carcinomas in relation to apoptosis. J. Pathol., *187:* 410–415, 1999.

54. Wosikowski, K., Regis, J. T., Robey, R. W., Alvarez, M., Buters, J. T. M., Gudas, J. M., and Bates, S. E. Normal p53 status and function despite the development of drug resistance in human breast cancer cells. Cell Growth Differ., *6:* 1395–1403, 1995.

55. Srinivasan, A., Li, F., Wong, A., Kodandapani, L., Smidt, R. Jr., Krebs, J. F., Fritz, L. C., Wu, J. C., and Tomaselli, K. J. Bcl-xL functions downstream of caspase-8 to inhibit Fas- and tumor necrosis factor receptor 1-induced apoptosis of MCF7 breast carcinoma cells. J. Biol. Chem., *273:* 4523–4529, 1998.

56. Keane, M. M., Ettenberg, S. A., Nau, M. M., Russell, E. K., and Lipkowitz, S. Chemotherapy augments TRAIL-induced apoptosis in breast cell lines. Cancer Res., *59:* 734–741, 1999.

57. Ludewig, B., Henn, V., Schröder, J. M., Graf, D., and Kroczek, R. A. Induction, regulation and function of soluble TRAP (CD40 ligand) during interaction of primary $CD4^+$ $CD45RA^+$ T cells with dendritic cells. Eur. J. Immunol., *26:* 3137–3143, 1996.

58. Younes, A., Snell, V., Consoli, U., Clodi, K., Zhao, S., Palmer, J. L., Thomas, E. K., Armitage, R. J., and Andreef, M. Elevated levels of biologically active soluble CD40 ligand in the serum of patients with chronic lymphocytic leukaemia. Br. J. Haematol., *100:* 135–141, 1998.

59. Kawakami, A., Eguchi, K., Matsuoka, N., Tsuboi, M., Koji, T., Urayama, S., Nakashima, T., Kawabe, Y., and Nagataki, S. Expression and function of Fas and Fas ligand on peripheral blood lymphocytes in normal subjects. J. Lab. Clin. Med., *132:* 404–13, 1998.

60. Aruga, E., Tanigawa, K., Aruga, A., Arai, H., Smith, J. W., II., Nickoloff, B. J., Nabel, G. J., and Chang, A. E. CD95-mediated tumor recognition by CD4+ effector cells in a murine mammary model. J. Immunother., *2:* 225–234, 2000.

61. Hillenbrand, E. E., Neville, A. M., and Coventry, B. J. Immunohistochemical localization of CD1a-positive putative dendritic cells in human breast tumours. Br. J. Cancer, *79:* 940–944, 1999.

62. Ravaioli, A., Bagli, L., Zucchini, A., and Monti, F. Prognosis and prediction of response in breast cancer: the current role of the main biological marker. Cell Prolif., *31:* 113–126, 1998.